



## Performance Evaluation of Heavy Metal Removal through Vertical Scale Bed Adsorption Process

R. Santhosh Kumar<sup>1\*</sup>, S. Kalaiselvi<sup>2</sup>

<sup>1</sup>HOD, Department of Civil Engineering, Vinayaka Mission's Kirupananda Variyar Engineering College, Vinayaka Mission's Research Foundation (DU).

<sup>2</sup>Assistant professor, Department of Civil Engineering, Sona College of Technology, Salem

\*Corresponding author: R. Santhosh Kumar, HOD, Department of Civil Engineering, Vinayaka Mission's Kirupananda Variyar Engineering College, Vinayaka Mission's Research Foundation (DU), Email: santhoshbala146@yahoo.com

Submitted: 12 April 2023; Accepted: 17 May 2023; Published: 06 June 2023

### ABSTRACT

The removal of congo red dye was found to be 99.9% removal at the optimum contact time 130 minutes at pH4 of the synthetic solution at a dosage of 6g/1000ml and at an agitation rate of 150rpm. From the design perspective the results were subjected to modeling of two domains, isotherm (Langmuir, Freundlich and Temkin) modeling and kinetic (Pseudo First order, Pseudo Second order and Intra particle Diffusion) modeling. Further after the adsorption studies post characterization was carried out on the nanoparticles using Field emission gun scanning electron microscopy – EDAX analysis, FTIR and TEM analysis. From the observation of the results it was confirmed that both lead and zinc has been adsorbed to cobalt ferrite and manganese ferrite nanoparticles in significant amount. Regeneration studies has been attempted for the Vertical Scale Bed Removal from the cobalt ferrite nanoparticles by showing the variation in time of contact and the normality of sodium hydroxide and it was noted that the re-extraction of the contaminant was found to be linear with the above operating parameters. To check the efficiency of the selected adsorbent the continuous mode Vertical Scale Bed studies were carried out for synthetic lead, zinc and congo red dye solutions by varying bed depth and flow rate.

**Keywords:** *Vertical Scale Bed, Heavy Metal Adsorption, Stimulation Analysis*

### INTRODUCTION

A fixed bed Vertical Scale Bed is used most commonly for contacting wastewater with the adsorbent. Fixed bed Vertical Scale Beds can be operated singly, in series, or in parallel. The advantage of a down flow design is that adsorption of organics and filtration of suspended solids is accomplished in a single step. Although up flow fixed-bed reactors have been used, down flow beds are used more

commonly to lessen the chance of accumulating particulate material in the bottom of the bed, where the particulate material would be difficult to remove by backwashing. If soluble organic material is not maintained at a high level, more frequent regeneration of the adsorbent may be required. Lack of consistency in pH, temperature, and flow rate may also affect performance of contactors.

### ***Metal Adsorption Process***

The fixed bed Vertical Scale Bed was fabricated using pyrex glass tube of 2.0 cm inner diameter and 20.0 cm height. The sampling ports were provided at four different depths to facilitate collection of samples. The Vertical Scale Bed performance of Pb(II), Zn(II) and congo red dye adsorption onto nanosorbents Cobalt ferrite and manganese ferrite were studied at different bed depths of 3cm, 6cm, 9cm, and 12cm. The flow rate of 5ml/minute was maintained throughout for the heavy metals whereas for Congo red dye the Vertical Scale Bed was operated at 5ml/min and 10ml/min. The Vertical Scale Bed was packed with the adsorbent for a total depth of 16cm. The metal and dye solutions were introduced into the Vertical Scale Bed bed by the gravity flow and the desirable flow rate were adjusted. Samples were collected from all the ports at regular interval of 10 minutes and analyzed for residual lead & zinc and congo red dye concentration. The experiments were conducted till the adsorbent gets exhausted.

The study also focus on the feasibility of using Thomas model and Yoon Nelson model to predict the performance of an adsorber bed packed with the nano structured adsorbent. Further simulation study in MATLAB using the concept of Feed Forward network and regression analysis using SPSS software was carried out for Congo red dye Vertical Scale Bed studies using cobalt ferrite nanoparticles as an adsorbent at a flow rate of 10ml/min.

### ***Lead And Zinc Removal From Its prepared Synthetic Source Using Cobalt Ferrite And Manganese Ferrite nanoparticles***

#### ***Effect of Bed Height – Lead Removal Using Cobalt Ferrite Nanoparticles***

In order to find out the effect of bed height on the breakthrough curve, the adsorbate solution having Lead concentration 50mg/L, pH 5.19 flow rate 5mL/min was passed through the adsorption Vertical Scale Bed by varying the bed height. Figure 5.1 presents the performance of breakthrough curves at bed heights of 3, 6, 9, and 12cm.

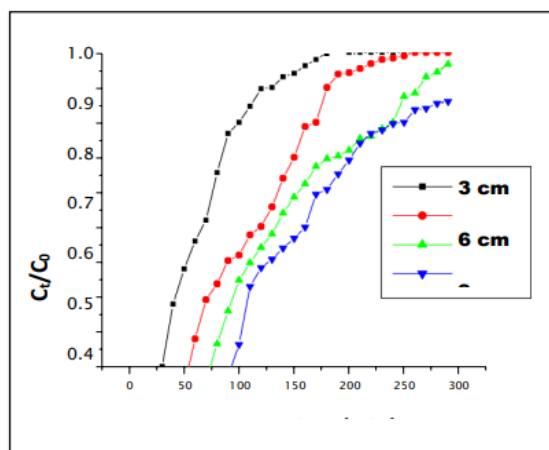


**FIGURE 1:** Effect of bed height on the breakthrough curve

It is evident from the Figure 5.1 that the steepness of the breakthrough curve was a function of bed height. With increase in bed height, the throughput volume was increased which might be due to higher contact time. At a relatively lower contact time, the curve was steeper showing the faster exhaustion of the bed. The higher uptake of Pb (II) was observed at the beginning of the fixed-bed Vertical Scale Bed, but the concentration of Pb (II) in the effluent rapidly increased after breakthrough volume or breakthrough time. The upper bed depth gets saturated earlier than lower bed depth. As can be seen in Figure 5.1, the breakthrough volume was 102, 202, 302 and 360 ml at bed depths of 3, 6, 9 and 12 cm, respectively. The breakthrough curve followed a characteristic „S“ shape profile which was associated with the size of the cobalt ferrite nanoparticles and its unique structural arrangement.

#### ***Application of Thomas Model***

The experimental data were fitted to the Thomas model to determine the Thomas rate constant ( $k_{TH}$ ) and maximum solid phase concentration ( $q_e$ ). The  $k_{TH}$  and  $q_e$  value were calculated by plotting  $\ln(C_0/C_0 - C_t)$  against „ $t$ “ using values from the Vertical Scale Bed experiments. From the regression coefficient and other statistical parameters, it is concluded that the experimental data fitted well to the Thomas model.  $k_{TH}$  and  $q_e$  values decreased with increase in bed height. The well fit of the experimental data on to the Thomas model indicated that the external and internal diffusion were not the rate limiting steps

(Figure 5.2).

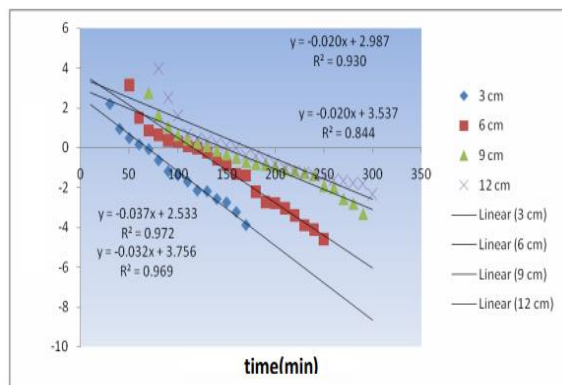


**FIGURE 2:** Experimental and theoretical breakthrough curve from Thomas Model at different bed height

**Application of Yoon Nelson model**

A simple theoretical model developed by Yoon – Nelson was applied to investigate the breakthrough behavior of Lead on the cobalt ferrite nanoparticles. The values of „ $K_{YN}$ ” and „ $\tau$ ” were estimated from the plot between  $\ln(C_0/C_0 - C_t)$  versus „ $t$ ” using values from Vertical Scale Bed experiments at different bed heights. The values of “ $K_{YN}$ ” were found to decrease with increase in bed height, whereas the corresponding values of „ $\tau$ ” increased Figure 3.

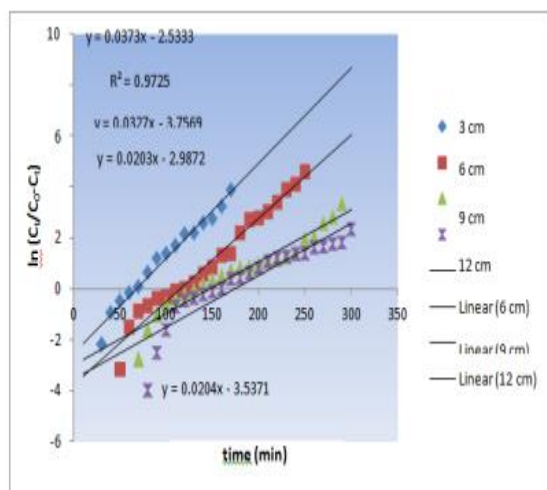


**FIGURE 3:** Experimental and theoretical breakthrough curve from Yoon Nelson Model at different bed height

**Effect of Bed height - Lead removal using Manganese ferrite nanoparticles**

In order to find out the effect of bed height on the breakthrough curve, the adsorbate solution

having Lead concentration 50mg/L, pH 5.19 flow rate 5mL/min was passed through the adsorption Vertical Scale Bed by varying the bed height. Figure 5.4 presents the performance of breakthrough curves at bed heights of 3, 6, 9, and 12cm. It is evident that the steepness of the breakthrough curve was a function of bed height. With increase in bed height, the throughput volume was increased which might be due to higher contact time. At a relatively lower contact time, the curve was steeper showing the faster exhaustion of the bed. The higher uptake of Pb (II) was observed at the beginning of the fixed-bed Vertical Scale Bed, but the concentration of Pb (II) in the effluent rapidly increased after breakthrough volume or breakthrough time. The upper bed depth gets saturated earlier than lower bed depth. As can be seen, the breakthrough volume was 30, 52, 102 and 170 ml at bed depths of 3,6, 9 and 12 cm, respectively Figure 4.

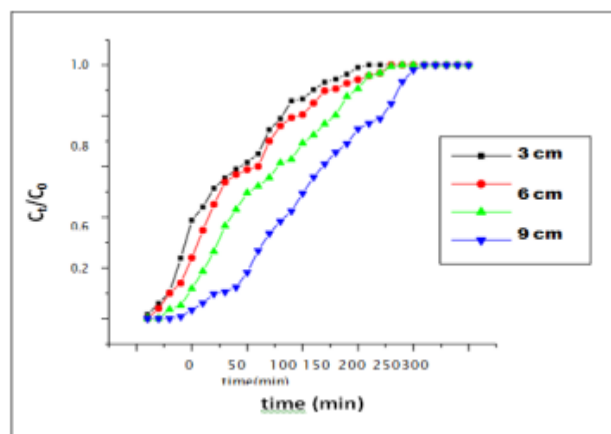


**FIGURE 4:** Effect of bed height on the breakthrough curve

**Application of Thomas Model**

The experimental data were fitted to the Thomas model to determine the Thomas rate constant ( $k_{TH}$ ) and maximum solid phase concentration ( $q_e$ ). The  $k_{TH}$  and  $q_e$  value were calculated by plotting  $\ln(C_0/C_0 - C_t)$  against „ $t$ ” using values from the Vertical Scale Bed experiments. From the regression coefficient and other statistical parameters, it is concluded that the experimental data fitted well to the Thomas model.  $k_{TH}$  and  $q_e$  values decreased with increase in bed height. The well fit of the experimental data on to the Thomas model indicated that the external and internal diffusion were not the rate limiting steps Figure 5.

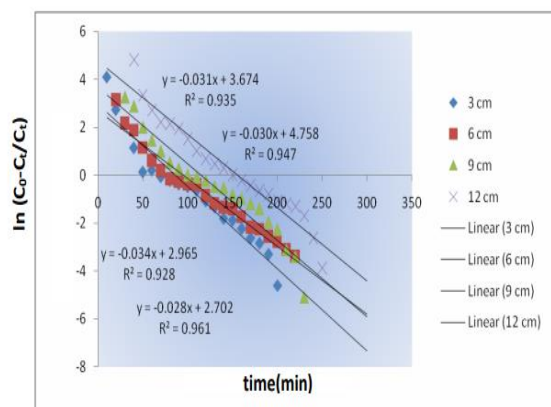


**FIGURE 5:** Experimental and theoretical breakthrough curve from Thomas Model at different bed height

**Application of Yoon Nelson model**

A simple theoretical model developed by Yoon – Nelson was applied to investigate the breakthrough behavior of Lead on the manganese ferritenanoparticles. The values of  $K_{YN}$  and  $\tau$  were reestimated from the plot between  $\ln(C_t/C_0 - C_t)$  versus  $t$  is using values from Vertical Scale Bed experiments at different bed heights. The values of “ $K_{YN}$ ” were found to decrease with increase in bed height, whereas the corresponding values of  $\tau$  increased Figure 5.6.

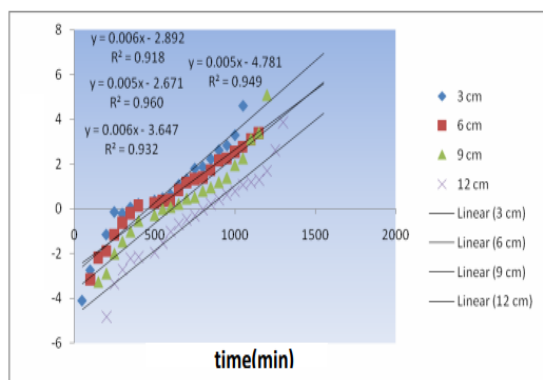


**FIGURE 6:** Experimental and theoretical breakthrough curve from Yoon Nelson Model at different bed height

**Effect of Bed Height - Zinc Removal Using Cobalt Ferrite Nanoparticles**

In order to find out the effect of bed height on the breakthrough curve, the adsorbate solution having Zinc concentration 50mg/L, pH 5.19 flow rate 5mL/min was passed through the adsorption

Vertical Scale Bed by varying the bed height. Figure 7 presents the performance of breakthrough curves at bed heights of 3, 6, 9, and 12cm.

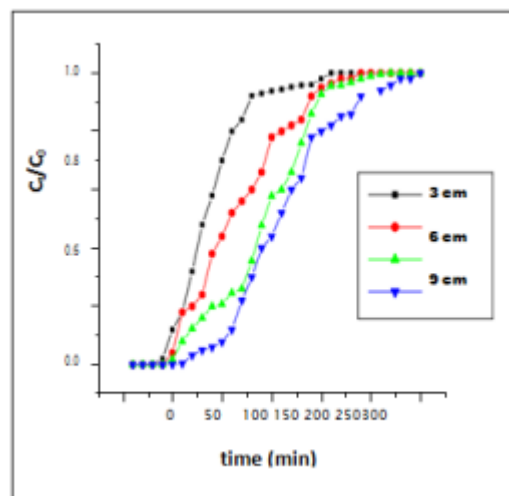


**FIGURE 7:** Effect of bed height on the breakthrough curve

It is evident from the Figure 7 that the steepness of the breakthrough curve was a function of bed height. With increase in bed height, the throughput volume was increased which might be due to higher contact time. At a relatively lower contact time, the curve was steeper showing the faster exhaustion of the bed. The higher uptake of Zn (II) was observed at the beginning of the fixed-bed Vertical Scale Bed, but the concentration of Zn (II) in the effluent rapidly increased after breakthrough volume or breakthrough time. The upper bed depth gets saturated earlier than lower bed depth. As can be seen in Figure 7, the breakthrough volume was 210, 270, 330 and 590 ml at bed depths of 3, 6, 9 and 12 cm, respectively.

**Application of Thomas Model**

The experimental data were fitted to the Thomas model to determine the Thomas rate constant ( $k_{TH}$ ) and maximum solid phase concentration ( $q_e$ ). From the regression coefficient and other statistical parameters, it is concluded that the experimental data fitted well to the Thomas model.  $k_{TH}$  and  $q_e$  values decreased with increase in bed height. The well fit of the experimental data on to the Thomas model indicated that the external and internal diffusion were not the rate limiting steps Figure 5.8.



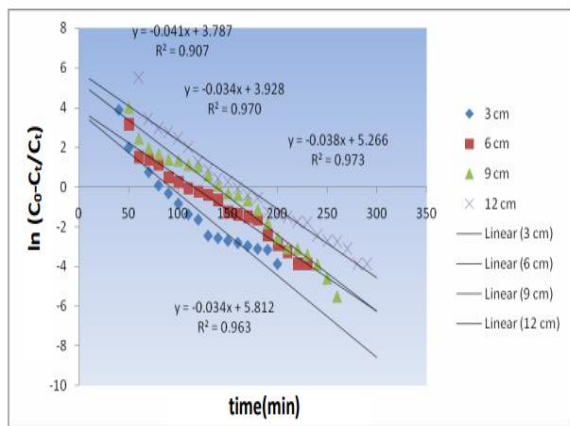


**FIGURE 8:** Experimental and theoretical breakthrough curve from Thomas Model at different bed height

**Application of Yoon Nelson model**

A simple theoretical model developed by Yoon – Nelson was applied to investigate the breakthrough behavior of zinc on the cobalt ferrite nanoparticles. The values of „ $K_{YN}$ ” and „ $\tau$ ” were estimated from the plot (Figure 5.9) between  $\ln(C_t/C_0 - C_t)$  versus „ $t$ ” using values from column experiments at different bed heights. The values of “ $K_{YN}$ ” were found to decrease with increase in bed height, whereas the corresponding values of „ $\tau$ ” increased.

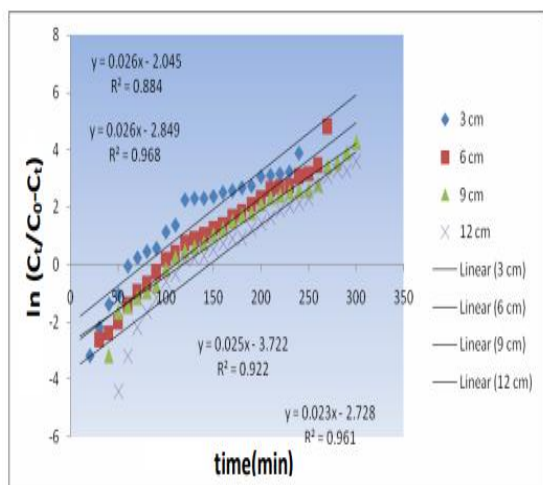


**FIGURE 9:** Experimental and theoretical breakthrough curve from Yoon Nelson Model at different bed height

**Effect of Bed Height – Zinc Removal Using Manganese Ferrite Nanoparticles**

In order to find out the effect of bed height on the breakthrough curve, the adsorbate solution

having Zinc concentration 50mg/L, pH 5.19 flow rate 5mL/min was passed through the adsorption Vertical Scale Bed by varying the bed height. Figure 5.10 presents the performance of breakthrough curves at bed heights of 3, 6, 9, and 12cm. It is evident from the Figure 10 that the steepness of the breakthrough curve was a function of bed height. With increase in bed height, the throughput volume was increased which might be due to higher contact time. At a relatively lower contact time, the curve was steeper showing the faster exhaustion of the bed. The higher uptake of Zn (II) was observed at the beginning of the fixed-bed Vertical Scale Bed, but the concentration of Zn (II) in the effluent rapidly increased after breakthrough volume or breakthrough time. The upper bed depth gets saturated earlier than lower bed depth. As can be seen in Figure 5.10, the breakthrough volume was 150, 230, 230 and 350 ml at bed depths of 3, 6, 9 and 12 cm, respectively.

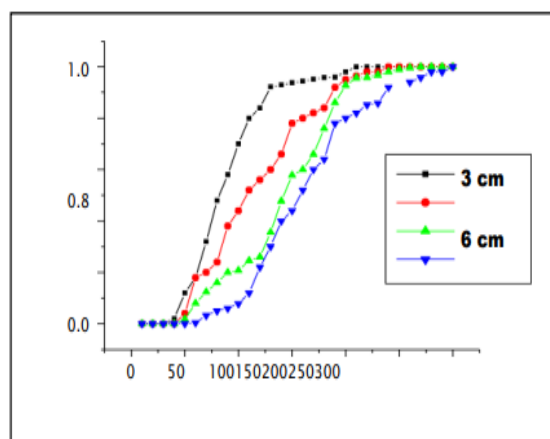


**FIGURE 10:** Effect of bed height on the breakthrough curve

**Application of Thomas Model**

The experimental data were fitted to the Thomas model to determine the Thomas rate constant ( $k_{TH}$ ) and maximum solid phase concentration ( $q_e$ ). The  $k_{TH}$  and  $q_e$  value were calculated by plotting  $\ln(C_0/C_0 - C_t)$  against „ $t$ ” using values from the Vertical Scale Bed experiments. From the regression coefficient and other statistical parameters, it is concluded that the experimental data fitted well to the Thomas model.  $k_{TH}$  and  $q_e$  values decreased with increase in bed height. The well fit of the experimental data on to the Thomas model indicated that the external and internal diffusion were not the rate limiting steps Figure 11.

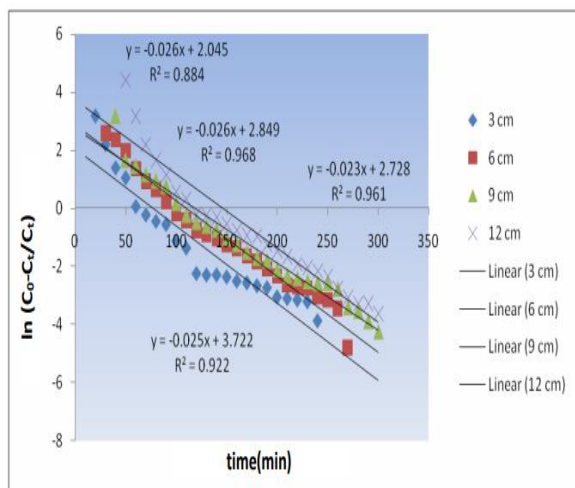


**FIGURE 11:** Experimental and theoretical breakthrough curve from Thomas Model at different bed height

**Application of Yoon Nelson model**

A simple theoretical model developed by Yoon – Nelson was applied to investigate the breakthrough behavior of zinc on the manganese ferrite nanoparticles. The values of „ $K_{YN}$ ” and „ $\tau$ ” were estimated from the plot between  $\ln(C_t/C_0 - C_t)$  versus „ $t$ ” using values from Vertical Scale Bed experiments at different bed heights. The values of „ $K_{YN}$ ” and „ $\tau$ ” were found to decrease with increase in bed height, Figure 12.

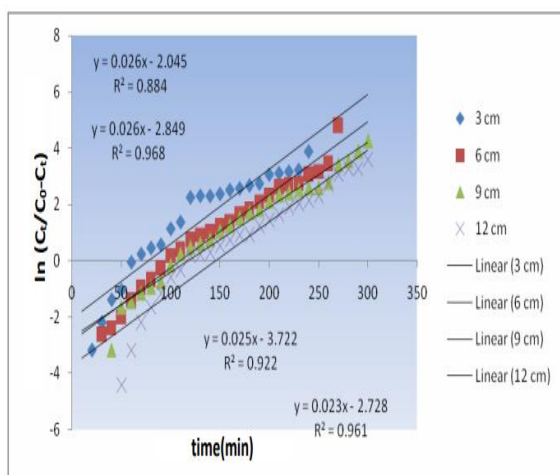


**FIGURE 12:** Experimental and theoretical breakthrough curve from Yoon Nelson Model at different bed height

**Congo Red Dye Vertical Scale Bed Studies Using Cobalt Ferritenanoparticles Influence of the Combination of Bed Height and Flow Rate of the Congo Red Dye Solution**

The results showed that the shape and gradient of the breakthrough curve was slightly different with the variation in bed depth. The higher uptake of Congo red dye was observed at the beginning of the fixed-bed Vertical Scale Bed, but the concentration of Congo red dye in the effluent rapidly increased after breakthrough volume. The upper bed depth gets saturated earlier than lower bed depth. At a flow rate of 5mL/min the breakthrough volume was 270 ml, 360 ml, 540 ml and 640ml at the bed depth of 3, 6, 9 and 12 cm, respectively. The breakthrough time was 52, 72, 102 and 122 minutes at the bed depth of 3, 6, 9, and 12cm respectively. The bed capacity exhausted at 950 ml, 1050 ml, 1150 ml and 1350 ml for bed depth of 3, 6, 9, 12 cm respectively.

At a flow rate of 10mL/minThe breakthrough volume was 102 ml, 252 ml, 273 ml and 356 ml at the bed depth of 3, 6, 9 and 12 cm, respectively. The bed capacity gets exhausted at 1000ml, 1040ml, 1230ml and 1710ml for bed depth of 3, 6, 9 and 12 cm. The breakthrough time was 16, 24, 28 and 36 minutes at the bed depth of 3, 6, 9, and 12cm respectively. It was observed that breakthrough generally occurred faster with higher flow rate. The reason is that at higher flowrate, the rate of mass transfer increased, thus the amount congo red dye adsorbed onto the unit bed height (mass transfer zone) increased. In addition, the adsorption capacity was lower as due to insufficient residence time of the solute in the Vertical Scale Bed and diffusion of the solute into the pores of the adsorbent, therefore the solute left the Vertical Scale Bed before equilibrium occurred (Figure 5.13, Figure5.14).

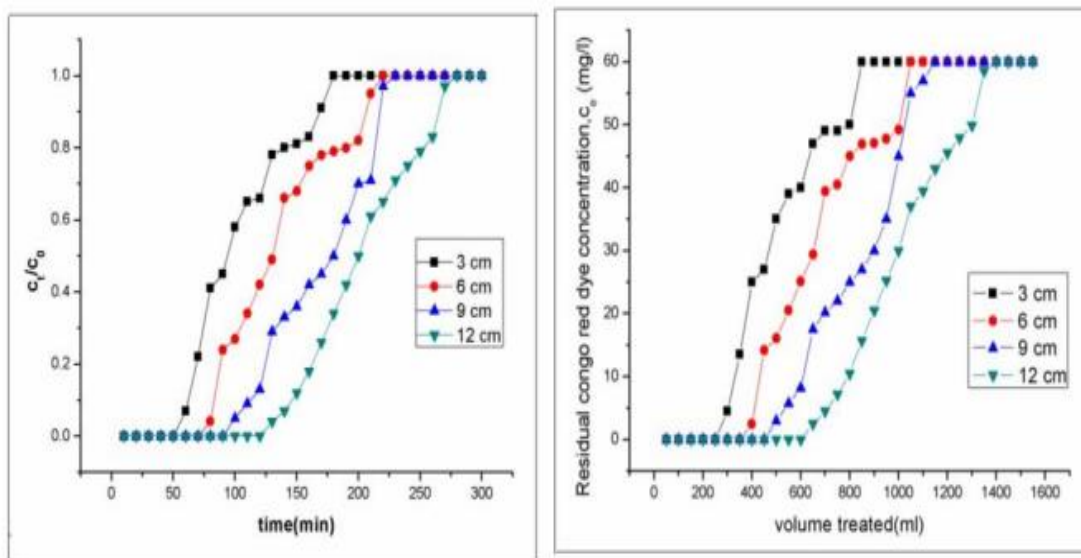


**FIGURE 13:** Combination of the effect of bed height and flow rate on the breakthrough curve for the flow rate of 5ml/min

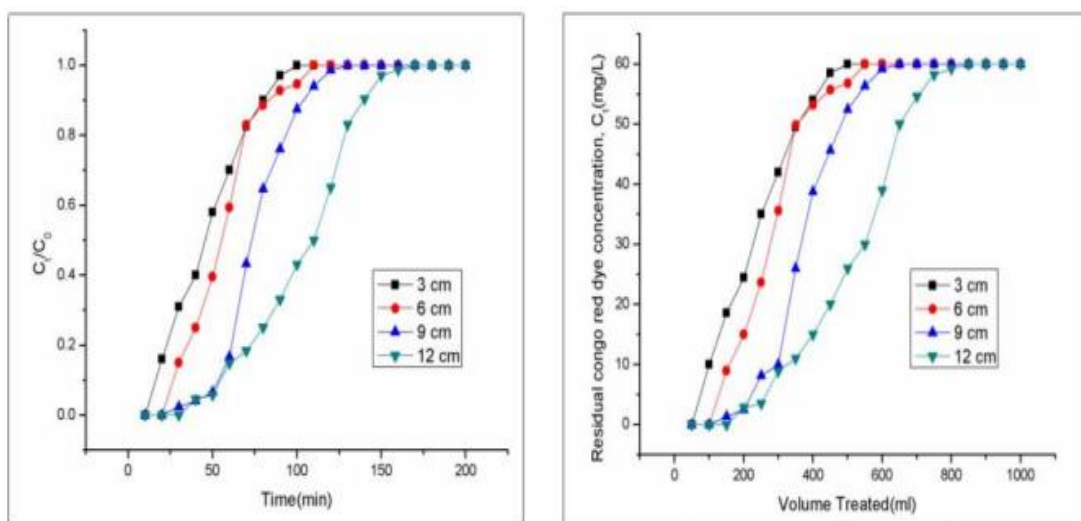


**FIGURE 14:** Combination of the effect of bed height and flow rate on the breakthrough curve for the flow rate of 10ml/min

**Application of Thomas Model**

The experimental data were fitted to the Thomas model to determine the Thomas rate constant ( $k_{TH}$ ) and maximum solid phase concentration ( $q_e$ ). The  $k_{TH}$  and  $q_e$  value were calculated by plotting  $\ln(C_0/C_0 - C_t)$  against „ $t$ “ using values from the Vertical Scale Bed experiments. From the regression coefficient and other statistical

parameters, it is concluded that the experimental data fitted well to the Thomas model.  $k_{TH}$  and  $q_e$  values decreased with increase in bed height. The well fit of the experimental data on to the Thomas model indicated that the external and internal diffusion were not the rate limiting steps Figure 15 and Figure 16.

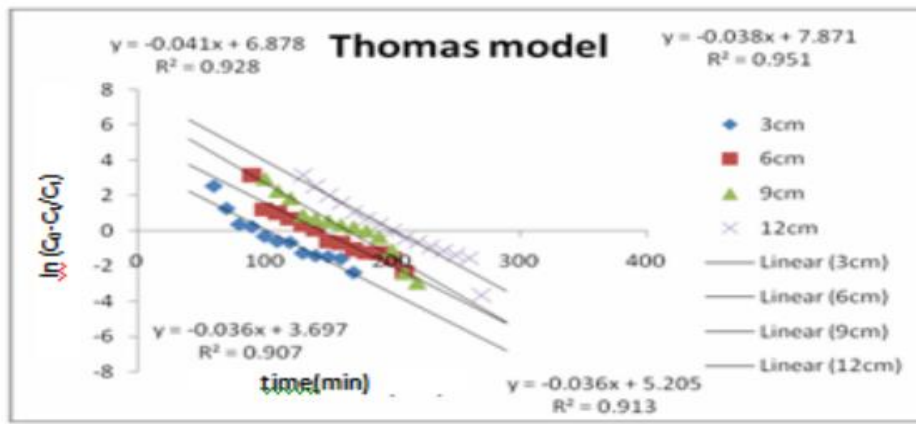


**FIGURE 15:** Experimental and theoretical breakthrough curve from Thomas Model at a flow rate of 5mL/min

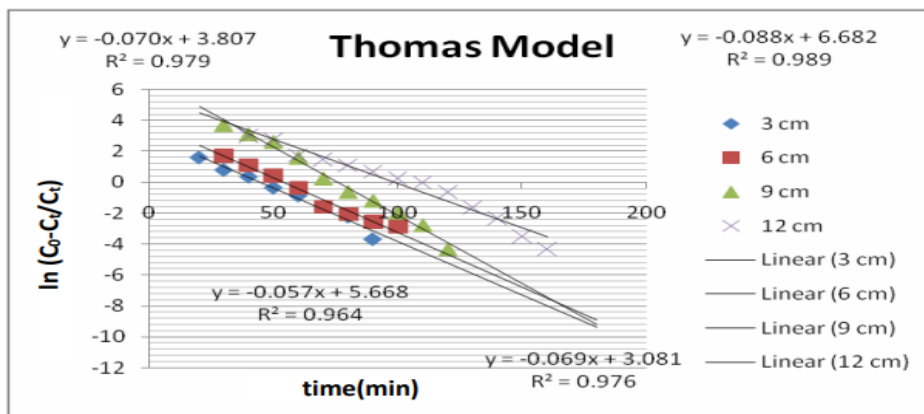


**FIGURE 16:** Experimental and theoretical breakthrough curve from Thomas Model at a flow rate of 10mL/min

**Application of Yoon-Nelson Model**

A simple theoretical model developed by Yoon – Nelson was applied to investigate the break through behavior of congo red dye on the cobalt ferrite nanoparticles. The values of „K<sub>YN</sub>” and „τ” were estimated from the plot between ln (C<sub>i</sub>/C<sub>0</sub>-

C<sub>t</sub>) versus „t” using values from Vertical Scale Bed experiments at different bed heights. The values of “K<sub>YN</sub>” and „τ” were found to increase with increase in bed height at both the flow rates, Figure 5.17 and Figure 5.18.

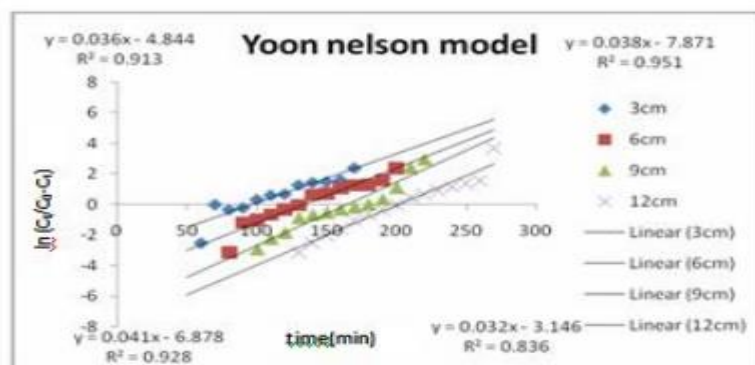


**FIGURE 17:** Experimental and theoretical breakthrough curve from Yoon-Nelson Model at a flow rate of 5mL/min



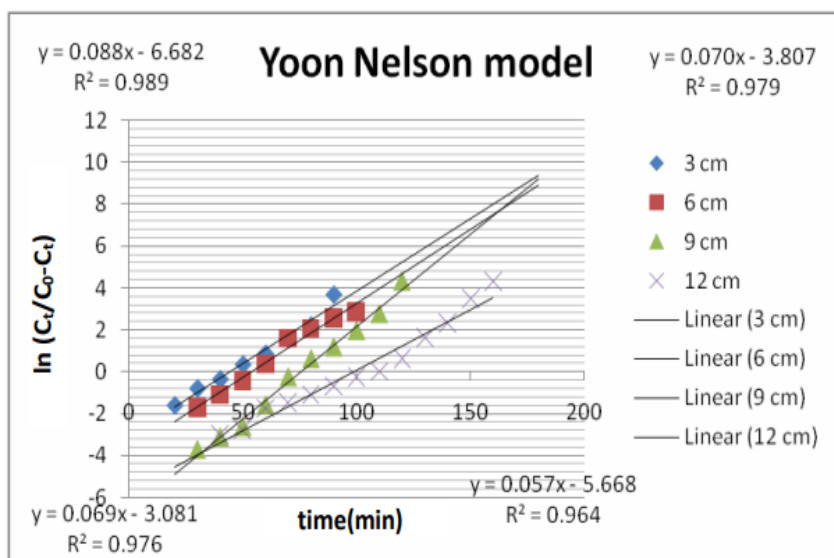


**FIGURE 18:** Experimental and theoretical breakthrough curve from Yoon-Nelson Model at a flow rate of 5mL/min

**TABLE 1:** Breakthrough time, and breakthrough volume for lead absorption using cobalt ferrite nanoparticles and manganese ferrite nanoparticles

Process Parameters		Adsorbate: Lead			
Flow rate :5mL/min		Adsorbent: Cobalt ferrite Nanoparticles		Adsorbent : Manganese Ferrite Nanoparticles	
Bed Depth (cm)	Breakthrough time (min)	Breakthrough volume (mL)	Breakthrough time (min)	Breakthrough volume (mL)	
3	22	102	8	30	
6	43	202	12	52	
9	64	302	23	102	
12	72	360	34	170	

**TABLE 2:** Breakthrough time and breakthrough volume for Zinc adsorption using Cobalt ferrite nanoparticles and Manganese ferrite nanoparticles

Process Parameters		Adsorbate: Zinc			
Flow rate :5mL/min		Adsorbent: Cobalt ferrite Nanoparticles		Adsorbent : Manganese Ferrite Nanoparticles	
Bed Depth (cm)	Breakthrough time (min)	Breakthrough volume (mL)	Breakthrough time (min)	Breakthrough volume (mL)	
3	41	210	32	150	
6	54	270	44	230	
9	65	330	45	230	
12	105	590	71	350	

**TABLE 3:** Breakthrough time and breakthrough volume for Congo red dye adsorption using Cobalt ferrite nanoparticles at a flow rate of 5mL/min

Process Parameters	Adsorbate: Congo Red Dye	
Flow rate :5mL/min	Adsorbent: Cobalt ferrite Nanoparticles	
Bed Depth (cm)	Breakthrough time (min)	Breakthrough volume (mL)
3	52	270
6	72	360
9	102	540
12	122	640

**TABLE 4:** Breakthrough time and breakthrough volume for Congo red dye adsorption using Cobalt ferrite nanoparticles at a flow rate of 10mL/min

Process Parameters	Adsorbate: Congo Red Dye	
Flow rate :10mL/min	Adsorbent: Cobalt ferrite Nanoparticles	
Bed Depth (cm)	Breakthrough time (min)	Breakthrough volume (mL)
3	16	102
6	24	252
9	28	273
12cm	36	356

**TABLE 5:** Thomas model constants for adsorption of lead and zinc using cobalt ferrite and manganese ferrite nanoparticles

Waste treated	Adsorbent	Bed depth (cm)	K <sub>TH</sub> (mL/min.mg)	q <sub>e</sub> (mg/g)	R <sup>2</sup>
Lead	Cobalt ferrite	3	0.00074	1.55	0.972
		6	0.00064	1.33	0.969
		9	0.0004	1.13	0.930
		12	0.0004	1.004	0.844
	manganese ferrite	3	0.00068	3.35	0.928
		6	0.00056	1.855	0.961
		9	0.00062	1.519	0.935
		12	0.0006	1.525	0.947
Zinc	Cobalt ferrite	3	0.00082	2.099	0.907
		6	0.00068	1.312	0.970
		9	0.00076	1.049	0.973
		12	0.00068	0.970	0.963
	manganese ferrite	3	0.00052	3.025	0.884
		6	0.00052	2.107	0.968
		9	0.00046	1.52	0.961
		12	0.0005	1.43	0.922

**TABLE 6:** Yoon Nelson model constants for adsorption of lead and zinc using cobalt ferrite and manganese ferrite nanoparticles

Waste treated	Adsorbent	Bed depth(cm)	K <sub>YN</sub> (L/min)	(min)	q <sub>e</sub> (mg/g)	R <sup>2</sup>
	Cobalt ferrite	3	0.037	68.45	1.55	0.972
		6	0.032	117.37	1.33	0.969
		9	0.020	149.35	1.13	0.930

Lead	Manganese ferrite	12	0.020	176.85	1.004	0.844
		3	0.006	482	18.53	0.918
		6	0.005	534.2	10.27	0.960
		9	0.006	607.83	7.79	0.932
Zinc	Cobalt ferrite	12	0.005	956.2	9.19	0.949
		3	0.041	92.36	2.09	0.907
		6	0.038	138.57	1.57	0.973
		9	0.034	115	0.87	0.970
	Manganese ferrite	12	0.034	170.94	0.97	0.963
		3	0.026	78.65	3.025	0.907
		6	0.026	109.57	2.107	0.970
		9	0.023	118.60	1.52	0.973
		12	0.025	148.88	1.43	0.963

**TABLE 7:** Thomas model constants for adsorption of Congo red dye using cobalt ferrite nanoparticles

Flow rate	Adsorbent	Bed depth (cm)	KTh (mL/min.mg)	q <sub>e</sub> (mg/g)	R <sup>2</sup>
5 mL/min	Cobalt ferrite	3	0.00060	2.8	0.907
		6	0.00060	1.8	0.913
		9	0.00068	1.4	0.928
		12	0.00063	1.3	0.951
10 mL/min	Cobalt ferrite	3	0.00115	2.4	0.976
		6	0.00116	1.4	0.979
		9	0.00146	1.3	0.989
		12	0.00095	1.2	0.964

**TABLE 8:** Yoon Nelson model constants for adsorption of Congo red dye using cobalt ferrite nanoparticles

Flow rate	Adsorbent	Bed depth (cm)	KYN (L/min)	(min)	q <sub>e</sub> (mg/g)	R <sup>2</sup>
5 mL/min	Cobalt ferrite	3	0.032	98.31	2.68	0.836
		6	0.036	134.55	1.75	0.913
		9	0.041	167.75	1.45	0.928
		12	0.038	207.13	1.32	0.951
10mL/min	Cobalt ferrite	3	0.069	44.65	2.43	0.976
		6	0.070	54.3	1.41	0.979
		9	0.088	75.93	1.32	0.989
		12	0.057	99.43	1.26	0.964

**Evolution Of Neural Network model**

Feed forward method is a systematic method for training multilayer artificial neural network. This is the most commonly used method, because of its relatively simple mathematical proof and good generalization capabilities. The difference between the network output and the expected output is determined .

absorbance, bed depth of the adsorbent, are taken as input parameters.

**Output Data**

The output parameter used is the percentage of removal measured from the experiments conducted in the laboratory under various conditions.

**Input Data**

Time of contact, Volume of the sample treated,

**Training the Network**

The purpose of training is to adjust the network weights such that the network produces the desired output in response to the input patterns. In the training stage the input and output patterns are presented to the neural network. The ANN is trained using the feed forward method. During

the training the input data (Time, volume absorbance and depth) and the corresponding output data (percentage of removal) were fed with shuffling to cover the entire operating range. Training data set for the adsorbent cobalt ferrite on the removal of Congo red dye is given in the following table:

**TABLE 9:** Network Training Data

S.No	Time	Volume (mL)	Absorbance	Depth (cm)	Percentage removal (Experimental) E (C <sub>e</sub> )
1	10	50	0.000	6	100
2	170	850	1.618	6	0
3	90	450	1.578	6	7.16
4	180	900	1.618	3	0
5	80	400	1.528	6	11.3
6	20	100	0.000	6	100
7	110	550	1.618	6	0
8	200	1000	1.618	9	0
9	140	700	1.565	12	9
10	120	600	1.105	12	35
11	100	500	1.618	3	0
12	90	450	1.595	3	2.5
13	170	850	1.618	9	0
14	10	50	0.000	3	100
15	170	850	1.618	3	0
16	150	750	1.589	12	3
17	50	250	0.032	12	94.1
18	70	350	1.492	3	17.5
19	10	50	0.000	9	100
20	60	300	0.194	12	85.1
21	80	400	1.532	3	54
22	100	500	0.728	12	56.6
23	40	200	0.025	9	95.8
24	200	1000	1.618	3	0
25	80	400	0.268	12	75
26	120	600	1.618	3	0
27	50	250	0.098	9	93.3
28	30	150	0.012	9	97.6
29	180	900	1.618	12	0
30	30	150	0.456	3	69
31	40	200	0.678	3	59.1
32	130	650	1.618	6	0
33	160	800	1.618	3	0
34	150	750	1.618	3	0
35	110	550	1.618	3	0
36	20	100	0.206	3	83.3
37	170	850	1.618	12	0
38	100	500	1.518	9	12.5
39	10	50	0	12	100
40	110	550	1.583	9	6
41	120	600	1.592	9	1.30
42	70	350	0.204	12	81.6
43	50	250	0.956	3	41.6



44	130	650	1.618	9	0
45	30	150	0	12	100
46	70	350	1.497	6	17
47	20	100	0	12	100
48	60	300	0.206	9	83.3
49	140	700	1.618	9	0
50	60	300	1.138	3	30
51	130	650	1.534	12	16.6
52	150	750	1.618	9	0
53	180	900	1.618	9	0
54	140	700	1.618	6	0
55	180	900	1.618	6	0
56	130	650	1.618	3	0
57	20	100	0	9	100

### Testing the Network

During testing, a new input pattern is presented and the output of the ANN is computed, which when compared with the target or actual output, should provide an excellent replica with minimum forecast error. The testing mode was selected and the number of layers and size of each layer from input to output were specified. The programme was run to generate the output. Outputs of ANN were compared with the

corresponding experimental output to determine the modelling efficiency. The results obtained from the feed forward network were compared with similar results obtained from the experimental observations. It was observed that the neural network output was found to be 85% nearer to the experimental output. The typical results obtained for the adsorbent Cobalt ferrite nanoparticle on the removal of Congo red dye is given in the table

**TABLE 10:** Network Testing Data

S.No	Time	Volume	Absorbance	Depth	E(C <sub>e</sub> )	N(C <sub>e</sub> )	Error E(C <sub>e</sub> )-N(C <sub>e</sub> )
1	160	800	1.618	6	0	0	0.00
2	30	150	0.194	6	85	72.01	12.99
3	40	200	0.028	12	95.3	81.1	14.20
4	200	1000	1.618	12	0	0	0.00
5	140	700	1.618	3	0	0	0.00
6	160	800	1.598	12	1	0.9	0.10
7	150	750	1.618	6	0	0	0.00
8	110	550	0.895	12	50	42.75	7.25
9	160	800	1.618	9	0	0	0.00
10	80	400	0.956	9	35.3	30	5.30
11	200	1000	1.618	6	0	0	0.00
12	90	450	0.56	12	66.6	57	9.60
13	60	300	0.958	6	24.4	20.02	4.38
14	120	600	1.618	6	0	0	0.00
15	90	450	1.245	9	23.8	20.1	3.70
16	100	500	1.585	6	5.3	4.5	0.80
17	40	200	0.389	6	75	64.01	10.99
18	70	350	0.685	9	56.6	48.01	8.59
19	50	250	0.664	6	61	51.95	9.05

### Regression Analysis

Further regression analysis were done for the Vertical Scale Bed studies of congo red dye

removal using cobalt ferrite nanoparticles using SPSS software where Time, volume, absorbance and depth were taken as independent parameters

and the removal were taken as dependent parameter. A regression equation was drawn relating the input and output parameters. From the regression analysis using SPSS software the regression coefficient value was found to be 0.986 which represents the SPSS output exhibited a close level of relation with the experimental output when comparing to the above mentioned Neural Network output.

Further, Regression analysis indicated that absorbance and the constant value 94.874 revealed a better level of significance 0.000 among the independent parameters. This constant value represents and indicates that the other unaccounted independent parameters like surface area of the adsorbent, coefficient of permeability etc could have played a vital role in determining the level often counter.

**TABLE 11:** A comparative table showing the experimental Results, MATLAB Result and SPSS Result

Time	Volume	Absorbance	Depth	E(C <sub>e</sub> )	N(C <sub>e</sub> )	SPSS OUTPUT
160	800	1.618	6	0	0	-0.032
30	150	0.194	6	85	72.01	84.89
40	200	0.028	12	95.3	81.1	96.76
200	1000	1.618	12	0	0	2.38
140	700	1.618	3	0	0	-1.24
160	800	1.598	12	1	0.9	2.433
150	750	1.618	6	0	0	-0.33
110	550	0.895	12	50	42.75	44.78
160	800	1.618	9	0	0	0.576
80	400	0.956	9	35.3	30	39.46
200	1000	1.618	6	0	0	1.167
90	450	0.56	12	66.6	57	65.07
60	300	0.958	6	24.4	20.02	38.13
120	600	1.618	6	0	0	-1.23
90	450	1.245	9	23.8	20.1	21.74
100	500	1.585	6	5.3	4.5	0.226
40	200	0.389	6	75	64.01	73.02
70	350	0.685	9	56.6	48.01	56.07
50	250	0.664	6	61	51.95	56.17

**TABLE 12:** Regression analysis for congo red dye adsorption using Cobalt Ferrite Nanoparticles

Model		Unstandardized Coefficients		Standardized Coefficients	t-value	Sig.	95% Confidence Interval for B	
		B	Std. Error	Beta			Lower Bound	Upper Bound
1	(Constant)	94.874	4.402	-	21.555	.000	85.543	104.205
	Time – X <sub>1</sub>	.006	.009	.047	.665	.516	-.013	.025
	Absorbance – X <sub>2</sub>	-.62.376	4.450	-1.029	-14.017	.000	-71.810	-52.943
	Depth – X <sub>3</sub>	.203	.433	.017	.470	.645	-.714	1.120

**TABLE 13:** Regression model Summary sheet

Model	R	R Square	Adjusted R Square	Std. Error of the Estimate	Change Statistics				
					R Square Change	F Change	df1	df2	Sig. Change

1	.993	.986	.983	4.3856554	.986	366.401	3	16	.000
Equation: Percentage Removal (Y)=94.874+0.006X <sub>1</sub> -62.376X <sub>2</sub> +0.203X <sub>3</sub>									

The coefficient of determination R<sup>2</sup> value shows that these variables when put together explain the variations of Y to the extent of 98.6%.

### CONCLUSIONS

The prepared cobalt ferrite nanoparticles were subjected for the removal of colour from the synthetic wastewater by considering congo red dye a contaminant of concern. The removal efficiency of 98% was achieved at the optimum contact time of 130minutes, adsorbent dosage was found to be 0.10 g/50ml, the optimum pH and initial lead concentration was found to be 4 and 60 mg/ L respectively. And finally the optimum speed was found to be 150 rpm. Langmuir and Temkin isotherms fitted well revealing that there is possible of homogenous multilayer adsorption. Pseudo first and second order kinetics gave a very good fit among the kinetics considered. The Vertical Scale Bed studies were carried out at different flow rates 5ml/min and 10ml/min. The Vertical Scale Bed data were subjected to Thomas and Yoon Nelson Model and it was observed that the adsorption capacity decreases from 2.8 mg/g to 1.3 mg/g and 2.4 mg/g to 1.2mg/g for the above two flow rates as the filtration depth increases.

### REFERENCES

1. Aadil Abbas, Shahzad Murtaza, Kashif Shahid, Muhammad Munir, Rabia Ayub & Saba Akber 2012, „Comparitive study of adsorptive removal of Congo red and Brilliant Green Dyes from water using Peanut Shell“, Middle –East Journal of Scientific Research, vol.11, no.6,pp.828-832.
2. Aadil Abbas, Shahzad Murtaza, Muhammad Munir, Tahreem Zahid, Noureen Abbas & Asim Mushtaq 2011, „Removal of Congo red from aqueous solutions with Raphanus sativus Peels and Activated carbon : A comparative study“, American Eurasian Journal of Agricultural and Environmental Sciences, vol.10, no.5,pp.802-809.
3. Abbas Afkhami & Razieh Moosavi 2010, „Adsorptive removal of Congo red, a carcinogenic textile dye, from aqueous solutions by maghemite nanoparticles“, Journal of Hazardous Materials, vol.174, pp.398-403.
4. Agnes Bee, Delphine Talbot, Sebastien Abramson & Vincent Dupuis 2011, „Magnetic alginate beads for Pb(II) ions removal from wastewater“, Journal of Colloid and Interface Science, vol.362,pp.486- 492.
5. Alemayehu Abebaw Mengistie, Siva Rao, T, Prasada Rao, AV& Malairajan Singanan 2008, „Removal of Lead(II)ions from aqueous solutions using activated carbon from Militia Ferruginea PlantLeaves“, Bulletin of the Chemical Society of Ethiopia, vol.22, no.3,pp.349-360.
6. Amit Bhatnagar & Minocha, AK 2006, „Conventional and non- conventional adsorbents for removal of pollutants from water – A review“, Indian Journal of Chemical Technology, vol.13,pp.203-217.
7. Andrea Kraus, Kunawoot Jainae, Faungfa Unob & Nipaka Sukpirom 2009, „Synthesis of MPTS cobalt ferrite nanoparticles and their adsorption properties in relation to Au(III)“, Journal of Colloid and Interface Science, vol.338,pp.359-365.
8. Ayşe Selek Murathan, Atila Murathan& Ahmet Yavuz Yücekutlu 2008, „Adsorption of Zinc ions on Fixed Bed“, Journal of International Environmental Application and Science, vol.3, no.5,pp.422-425.
9. Bandara,J,Morrison,C,Kiwi,J,Pulgarin,C&Perien ger,P1996,
10. „Degradation/decoloration of concentrated solutions of orange II. Kinetics and quantum yield for sunlight induced reactions via Fenton type reagents“, Journal of Photochemical and Photobiological, vol.99, pp.57-66.
11. Bogner, A, Jouneau , PH, Thollet, G, Basset, D& Gauthier, C 2007,„A history of scanning electron Microscopy developments: Towards „Wet-STEM“ imaging“, Micron, vol.38,pp.390-401.
12. Bottero, JY 1993, „Surface and textural heterogeneity of fresh hydrous ferric oxides in water and in dry state“, Journal of Colloids and Interface Science, vol.159,pp.45-52.
13. Bottero, JY, Cases, JM, Fiessinger, F & Piorier, JE 1980, „Studies of hydrolyzed aluminium chloride solutions“, 1. Nature of aluminium species and composition of aqueous solutions, Journal of Physical Chemistry, vol.84, no.22,pp.2933-2937.
14. Bottero, JY, Manceau, A, Villieras, F & Tchoubar, D 1994, „Structure and mechanisms of formation of FeOOH(Cl) polycations“, Langmuir, vol.10, no.1,pp.316-320.
15. Bottero, JY, Tchoubar, D, Cases, JM & Fiessinger, F 1982,
16. „Investigation of the hydrolysis of aqueous solutions of aluminium chloride“, 2. Natur and

- structure by small-angle X-ray scattering. *Journal of Physical Chemistry*, vol.86, no.18, pp.3667-3673.
17. Charif Gakwisiri, Nitin Raut, Amal Al-Saadi, Shinoona Al-Aisri & Abrar Al-Ajmi 2012, „A critical review of removal of Zinc from wastewater“, *Proceedings of the World Congress on Engineering*, ISBN :978-988-19251-3-8, vol.1.
  18. Chungsyng Lu & Huantsung Chiu 2006, „Adsorption of Zinc(II) from water with purified carbon nanotubes“, *Chemical Engineering Science*, vol.61, pp.1138-1145.
  19. Curl, RF, Smalley, RE, Kroto, HW, O'Brien, S & Heath, JR 2001,
  20. „How the news that we were not the first to conceive of Soccer ball C-60 got to us“, *Journal of Molecular Graphics & Modelling*, vol.19, no.2, pp.185-186.
  21. Dabrowski, A 2001, „Adsorption – From theory to practice“, *Advances in Colloidal and Interface Science*, vol.93, pp.135-224.
  22. David Hendricks 2011, „Adsorption“, *Fundamentals of Water Treatment Unit Processes*, pp.457-510.
  23. Di, ZC, Li, YH, Luan, ZK & Liang, J 2004, „Adsorption of chromium (VI) ions from water using carbon nanotubes“, *Adsorption Science and Technology*, vol.22, no.6, pp.467-474.
  24. Dilek (Yalcin) Duygu, Tulay Baykal, Đlkay Acikgoz & Kazım Yildiz 2009, „Fourier Transform Infrared (FT-IR) spectroscopy for biological studies“, *Gazi University Journal of Science*, vol.22, no.3, pp.117-121.
  25. Environmental Health Criteria 221 World health organization Geneva 2001, pp.1-349.
  26. Fannin, PC, Marin, CN, Malaescu, I, Stefu, N, Vlazan, P, Novaconi, S, Sfirioaga, P, Popescu, S & Couper, C 2010, „Microwave adsorbent properties of nanosized cobalt ferrite powders prepared by coprecipitation and subjected to different thermal treatments“, *Materials and Design*, vol.32, issue 3, pp.1600-1604.
  27. Flavio A Pavan, Silvio LP Dias, Eder C Lima & Edilson V Benvenuti 2008, „Removal of Congo red from aqueous solution by anilinepropylsilica xerogel“, *Dyes and Pigments*, vol.76, pp.64-69.
  28. Forgacs, E & Cserhati, T 2004, „Removal of synthetic dyes from wastewaters: a review“, *Environment International*, vol.30, pp.953-971.
  29. Gao, JF, Zhang, Q, Su, K & Wang, JH 2010, „Comparative biosorption of Yellow 2G and Reactive Brilliant Red K-2G onto inactive aerobic granules: simultaneous determination of two dyes by first-order derivative spectrophotometry and isotherm studies“, *Bioresource Technology*, vol.101, pp.5793-5801.
  30. Ghaedi, M, Ramazani, S & Roosta, M 2011, „Gold nanoparticle loaded activated carbon as novel adsorbent for the removal of Congo red“, vol.4, no.10, pp.1208-1217.
  31. Gholamreza Moussavi & Maryam Mahmoudi 2009, „Removal of azo and anthraquinone reactive dyes from industrial wastewaters using MgO nanoparticles“, *Journal of Hazardous Materials*, vol.168, pp.806-812.
  32. Gidlow, DA 2004, „In-Depth Review Lead toxicity“, *Occupational Medicine*, vol.54, pp.76-81.
  33. Glenn, JC 2006, „Nanotechnology: Future military environmental health considerations“, *Technological Forecasting and Social Change*, vol.73, no.2, pp.128-137.
  34. Gupta, SC & Kapoor, VK, *Fundamentals of Mathematical Statistics*, Sultan Chand and Sons ISBN:978-81-8054-528-3, pp.11.1-11.26.
  35. Gupta, VK & Suhas 2009, „Application of low cost adsorbents for dye removal – A review“, *Journal of Environmental Management*, vol.90, pp.2313-2342.
  36. Haider M Zwain, Mohammadtaghi Vakili & Irvan Dahlan 2014, „Waste material adsorbents for Zinc removal from wastewater: A comprehensive review“, *International Journal of Chemical Engineering*, pp.1-13.
  37. Hsieh, SH & Horng, JJ 2007, „Adsorption behaviour of heavy metal ions by carbon nanotubes grown on micro-sized Al<sub>2</sub>O<sub>3</sub> particles“, *Journal of University of Science and Technology*, vol.14, issue 1, pp.77-84.
  38. Igwe, JC, Ogunewe, DN & Abia, AA 2005, „Comparative adsorption of Zn(II), Cd(II), and Pb(II) ions from aqueous and non aqueous solution by maize cob and rice husk“, *African Journal of Biotechnology*, vol.4, no.10, pp.1113-1116.
  39. Iman Mobasherpour, Esmail Salahi & Aliasjodi 2014, „Research on the batch and fixed-bed column performance of red mud adsorbents for lead removal“, vol.2, issue 1, pp.83-96.
  40. Imran Ali 2012, „New Generation Adsorbents for Water treatment“, *Chemical Reviews*, vol.112, pp.5073-5091.
  41. Indra Deo Mall, Vimal Chandra Srivastava, Nitin Kumar Agarwal \* Indra Mani Mishra 2005, „Removal of Congo red from aqueous solution by bagasse flyash and activated carbon: Kinetic study and equilibrium isotherm analyses“, *Chemosphere*, vol.61, pp.492-501.
  42. Irfan Elahi, Rabab Zahira, Kiren Mehmood, Arifa Jamil & Nasir Amin 2012, „Co-precipitation synthesis, Physical and magnetic properties of manganese ferrite powder“, *African Journal of Pure and Applied Chemistry*, vol.6, no.1, pp.1-5.
  43. Jameel M Dhabab 2011, „Removal of Fe(II), Cu(II), Zn(II), and Pb(II) ions from aqueous solutions by duckweed“, *Journal of Oceanography and Marine Science*, vol. 2, no.1, pp.17-22.
  44. Jayaraj, R, Jeyasingh Thanaraj, P, Thillai



- Natarajan, S & Martin Deva Prasath, P 2011, „Removal of Congo red dye from aqueous solution using acid activated Eco-Friendly Low cost Carbon prepared from marine algae *Valoria bryopsis*“, *Journal of Chemical and Pharmaceutical Research*, vol.3, no.3, pp.389-396.
46. Jing Hu, Irene MC Lo & Guohua Chen 2007, „Comparitive study of various magnetic nanoparticles for Cr(VI) removal“, *Seperation and Purification Technology*, vol.56, pp.249-256.
47. Julija Volmajer Valh & Alenka Majcen Le Marechal 2009,
48. „Decoloration of textile wastewaters“, *Dyes and Pigments – New Research*, pp. 190-199.
49. Jyoti Sharma & Beena Janveja 2008, „A study on removal of Congo red dye from the effluents of Textile Industry using Rice Husk carbon activated by steam“, *Rasayan Journal of Chemistry*, vol.1, no.4, pp.936-942.
50. Khayat Sarkar, Z& Khayat Sarkar, F 2013, „Selective removal of lead(II) Ion from wastewater using superparamagnetic Monodispersed Iron oxide (Fe<sub>3</sub>O<sub>4</sub>) Nanoparticles as a effective adsorbent“, vol.9, no.2, pp.109-114.
51. Lenore S Clesceri, Arnold E Green berg & Andrew D Eaton 1998, *Standard Methods for the Examination of water and wastewater* 20th Edition, pp.3-21.
52. Liu, G 2005, „The preparation of Zn<sup>2+</sup> doped TiO<sub>2</sub> nanoparticles by sol-gel and solid phase reaction methods respectively and their photocatalytic activities“, *Chemosphere*, vol.59, no.9, pp.1367.
53. Lixia Wang, Jianchen Li, Yingqi Wang & Lijun Zhao 2012, „Adsorption capability for Congo red on nanocrystalline MFe<sub>2</sub>O<sub>4</sub> (M=Mn, Fe, Co, Ni) spinel ferrites“, *Chemical Engineering Journal*, vol.181, pp.72- 79.
54. Maaz, K, Arif Mumtaz, Hasanian, SK & Abdullah Ceylan 2007, „Synthesis and magnetic properties of Cobalt ferrite (CoFe<sub>2</sub>O<sub>4</sub>) nanoparticles prepared by Wet chemical route“, *Journal of Magnetism and Magnetic Materials*, vol.308, issue 2, pp.289-295.
55. Martin, CR & Mitchell, DT 1998, „Nanomaterials in analytical chemistry“, *Analytical Chemistry*, vol.70, no.9, pp.322A-327A